

Solubility of Carbon Dioxide in Liquid Mixtures of Water + [bmim][CH₃SO₄]

Jacek Kumełan, Álvaro Pérez-Salado Kamps, Dirk Tuma,[†] and Gerd Maurer*

Department of Mechanical and Process Engineering, University of Kaiserslautern, P.O. Box 3049, D-67653 Kaiserslautern, Germany

ABSTRACT: Experimental results are reported for the solubility of carbon dioxide in liquid mixtures of water and the ionic liquid 1-*n*-butyl-3-methylimidazolium methylsulfate ([bmim][CH₃SO₄]). Three (gas-free) solvent compositions were considered with mass fractions of [bmim][CH₃SO₄] of $w' \approx 0.15, 0.50,$ and 0.87 (mole fractions $x' \approx 0.013, 0.066,$ and 0.33). In the isothermal experimental series, the temperature was about (293, 333, and 373) K. The total pressure ranged up to about 10 MPa. The molality of carbon dioxide in the solvent mixture of (water + [bmim][CH₃SO₄]) (the mole fraction of carbon dioxide in the liquid) ranged up to approximately $1.64 \text{ mol} \cdot \text{kg}^{-1}$ (about 0.0332). The experimental results are used to determine Henry's constant of carbon dioxide in the liquid mixtures of (water + [bmim][CH₃SO₄]) as well as the partial molar volume of that gas at infinite dilution in those solvent mixtures. The phase equilibrium is described by applying an extension (to solvent mixtures) of Pitzer's molality scale-based equation for the Gibbs excess energy.

INTRODUCTION

Experimental data for the solubility of gases in ionic liquids as well as in solvent mixtures containing ionic liquids are not only important from an application-oriented point of view. They are also required to provide a database for the development of correlation methods and predictive tools such as molecular simulation.^{1,2} The present paper aims to contribute to such a database by dealing with the solubility of carbon dioxide in aqueous solutions of [bmim][CH₃SO₄]. As far as is known to the authors, no experimental information on the solubility of carbon dioxide in aqueous solutions of [bmim][CH₃SO₄] is available in the open literature. In addition, a vapor–liquid equilibrium (VLE) model is developed to correlate the gas solubility data over the whole range of solvent mixture composition, from pure water to the pure ionic liquid. That model resorts on a previously presented extension (to solvent mixtures)³ of the classical equation developed by Pitzer for the Gibbs excess energy of electrolyte solutions based on the molality scale.^{4,5}

EXPERIMENTAL SECTION AND RESULTS

Materials and Sample Pretreatment. Carbon dioxide (4.5, volume fraction ≥ 0.99995) was supplied by Messer Griesheim, a subsidiary of the Messer Group GmbH (Krefeld, Germany). The gas was used without further purification. The ionic liquid [bmim][CH₃SO₄] (CAS Registry No.: 401788-98-5, C₉H₁₈N₂O₄S, purity: HPLC peak area fraction ≥ 0.980 , dark yellow liquid, relative molar mass $M = 250.32$) was from Merck Solvent Innovation GmbH (Cologne, Germany). According to the specification of the supplier, the amount of halides (dimethyl sulfate) was below 0.1 (0.01) peak area percent. The sample was degassed and dried under vacuum over a period of two days to remove traces of volatile impurities. The water content of the sample was less than 0.001 mass fraction, as determined by Karl Fischer titration. Water was deionized and degassed before being used for preparing the aqueous mixtures. The solvent mixtures (typically about 1100 g) were prepared gravimetrically from the

degassed solvent components using a high-precision analytical balance (PR 5003, Mettler-Toledo GmbH, Giessen, Germany). A glass buret served as a sample container so that the mixture could be handled and introduced into the apparatus always under vacuum, and any moisture intrusion from the laboratory air was blocked. The uncertainty of the individual mass of a solvent was ± 0.1 g for the ionic liquid and ± 0.5 g for water. The mass fraction of the ionic liquid in the three gas-free solvent mixtures was $0.1501 \pm 0.0002, 0.4956 \pm 0.0004,$ and 0.8705 ± 0.0006 , respectively. After each series of measurements, the density of a sample of the liquid mixture from the view cell was determined using a vibrating-tube densimeter (see below) to check the solvent composition. All deviations were smaller than the accumulated uncertainty (from preparing the solvent mixtures and the density measurements).

Apparatus and Method. The setup of the gas solubility apparatus was the same as for the experiments with pure ionic liquids. For a detailed outline, the reader is referred to the latest papers of our publication series on gas solubility in different pure ionic liquids as well as to Kumełan's doctoral thesis.^{6–8} The experimental procedures and experimental uncertainties are comprehensively reported in those references. Therefore, we restrict to the basic workflow and amend the specific differences that result from the particular system investigated.

The experimental procedure can be characterized as follows: The pressure is measured which is required to dissolve a precisely known amount of gas in an also precisely known amount of solvent that fills a high-pressure thermostatted view cell.

The mass of carbon dioxide introduced into the cell was determined volumetrically, that is, from the known volume of the view cell (approximately 30 cm³) and the density of the gas,

Special Issue: Kenneth N. Marsh Festschrift

Received: May 16, 2011

Accepted: August 3, 2011

Published: August 22, 2011

Table 1. Density ρ /($\text{kg} \cdot \text{dm}^{-3}$) of Liquid Mixtures of Water (1) + [bmim][CH₃SO₄] (2) ($\Delta T = \pm 0.1$ K, $\Delta \rho = \pm 0.0001$ $\text{kg} \cdot \text{dm}^{-3}$)^a

w'_2	T/K					
	293.15	295.15	297.15	299.15	301.15	303.15
0.00	0.9983	0.9979	0.9974	0.9969	0.9963	0.9957
0.1501 \pm 0.0002	1.0258	1.0251	1.0244	1.0237	1.0229	1.0222
0.2002 \pm 0.0002	1.0359	1.0352	1.0344	1.0336	1.0328	1.0319
0.2991 \pm 0.0003	1.0561	1.0552	1.0543	1.0533	1.0523	1.0513
0.4993 \pm 0.0004	1.1002	1.0990	1.0977	1.0965	1.0952	1.0939
0.6519 \pm 0.0005	1.1349	1.1335	1.1322	1.1307	1.1294	1.1280
0.8012 \pm 0.0006	1.1694	1.1680	1.1666	1.1652	1.1638	1.1624
0.8701 \pm 0.0006	1.1848	1.1834	1.1821	1.1807	1.1793	1.1779
0.9325 \pm 0.0007	1.1982	1.1968	1.1955	1.1941	1.1928	1.1914
1.00	1.2117	1.2104	1.2091	1.2077	1.2064	1.2051

^a w'_2 = mass fraction of [bmim][CH₃SO₄] in the solvent mixture of (H₂O + [bmim][CH₃SO₄]).

Table 2. Experimental Results for the Solubility of Carbon Dioxide (3) in Water (1) + [bmim][CH₃SO₄] (2) at $w'_2 = 0.1501 \pm 0.0002$ ($x'_2 = 0.01255 \pm 0.00002$) ($\Delta T = \pm 0.1$ K)^a

T	m_3	p	V/\bar{m}_s
K	$\text{mol} \cdot \text{kg}^{-1}$	MPa	$\text{cm}^3 \cdot \text{kg}^{-1}$
293.1	0.2671 \pm 0.0013	0.785 \pm 0.021	984.5 \pm 3.0
	0.3922 \pm 0.0016	1.222 \pm 0.022	989.4 \pm 3.0
	0.5454 \pm 0.0020	1.737 \pm 0.023	995.6 \pm 3.1
	0.6691 \pm 0.0023	2.162 \pm 0.024	1000.7 \pm 3.1
	0.9228 \pm 0.0030	3.212 \pm 0.034	1011.3 \pm 3.1
	1.1746 \pm 0.0037	4.558 \pm 0.036	1023.7 \pm 3.2
333.1	0.1766 \pm 0.0011	1.159 \pm 0.024	1000.8 \pm 3.1
	0.2981 \pm 0.0013	1.995 \pm 0.025	1003.0 \pm 3.1
	0.4603 \pm 0.0017	3.255 \pm 0.035	1006.9 \pm 3.1
	0.5883 \pm 0.0020	4.345 \pm 0.037	1011.4 \pm 3.1
	0.7464 \pm 0.0024	5.809 \pm 0.040	1015.7 \pm 3.1
	0.8882 \pm 0.0028	7.579 \pm 0.043	1020.1 \pm 3.1
373.1	1.0539 \pm 0.0035	10.004 \pm 0.047	1024.4 \pm 3.1
	0.0885 \pm 0.0009	0.883 \pm 0.026	1023.1 \pm 3.1
	0.2114 \pm 0.0010	2.178 \pm 0.028	1026.0 \pm 3.2
	0.3264 \pm 0.0013	3.444 \pm 0.038	1029.1 \pm 3.2
	0.4468 \pm 0.0016	4.849 \pm 0.041	1034.6 \pm 3.2
	0.5799 \pm 0.0019	6.500 \pm 0.044	1038.3 \pm 3.2
	0.7181 \pm 0.0023	8.303 \pm 0.048	1043.5 \pm 3.2

^a T = temperature, w'_2 (x'_2) = mass fraction (mole fraction) of [bmim][CH₃SO₄] in the (gas-free) solvent mixture of (H₂O + [bmim][CH₃SO₄]), m_3 = molality of CO₂ in the liquid = amount of substance of CO₂ per kilogram of solvent mixture of (H₂O + [bmim][CH₃SO₄]), p = total pressure, V/\bar{m}_s = volume of the ternary liquid per mass of solvent mixture of (H₂O + [bmim][CH₃SO₄]).

which was calculated from readings for temperature and pressure according to the equation of state given by Span and Wagner⁹ as implemented in the software package "ThermoFluids".¹⁰ The mass of the solvent, that is, the mixture of (water + ionic liquid [bmim][CH₃SO₄]) filled into the cell was calculated from the volume displacement in a calibrated spindle press, which was

Table 3. Experimental Results for the Solubility of Carbon Dioxide (3) in Water (1) + [bmim][CH₃SO₄] (2) at $w'_2 = 0.4956 \pm 0.0004$ ($x'_2 = 0.06604 \pm 0.00010$) ($\Delta T = \pm 0.1$ K)^a

T	m_3	p	V/\bar{m}_s
K	$\text{mol} \cdot \text{kg}^{-1}$	MPa	$\text{cm}^3 \cdot \text{kg}^{-1}$
293.2	0.2365 \pm 0.0012	0.899 \pm 0.022	917.4 \pm 2.8
	0.4021 \pm 0.0016	1.580 \pm 0.023	924.3 \pm 2.8
	0.5613 \pm 0.0020	2.288 \pm 0.025	927.9 \pm 2.8
	0.6949 \pm 0.0023	2.945 \pm 0.034	930.7 \pm 2.8
	0.8631 \pm 0.0028	3.777 \pm 0.035	934.8 \pm 2.9
	1.0829 \pm 0.0034	5.221 \pm 0.038	942.1 \pm 2.9
333.2	0.1737 \pm 0.0010	1.124 \pm 0.024	937.3 \pm 2.9
	0.3535 \pm 0.0014	2.399 \pm 0.026	944.6 \pm 2.9
	0.5506 \pm 0.0019	3.821 \pm 0.037	950.6 \pm 2.9
	0.7417 \pm 0.0024	5.587 \pm 0.040	953.0 \pm 2.9
	0.9531 \pm 0.0030	7.801 \pm 0.044	962.4 \pm 2.9
	1.0835 \pm 0.0036	9.502 \pm 0.047	967.4 \pm 3.0
373.1	0.1350 \pm 0.0009	1.220 \pm 0.025	965.2 \pm 3.0
	0.2617 \pm 0.0011	2.424 \pm 0.027	969.7 \pm 3.0
	0.3955 \pm 0.0014	3.751 \pm 0.038	972.0 \pm 3.0
	0.5295 \pm 0.0018	5.092 \pm 0.041	977.6 \pm 3.0
	0.6808 \pm 0.0022	6.715 \pm 0.045	984.3 \pm 3.0
	0.8259 \pm 0.0026	8.428 \pm 0.048	988.5 \pm 3.0

^a See the footnote in Table 2.

used for transferring the solvent into the cell, and the solvent density. The density of the solvent mixtures was independently determined in the temperature region between (293 and 303) K using a vibrating-tube densimeter (DMA 4500 M, Anton Paar GmbH, Graz, Austria). The experimental results for the density of the solvent mixtures are given in Table 1. The temperature and pressure were determined with the same devices as described recently.^{6,7} Details are therefore not repeated here.

The experimental uncertainties of temperature and pressure, as well as the procedures for estimating the experimental uncertainties of the masses of the solute gas and of the solvent introduced into the cell, of the view-cell volume, and so forth, were exactly the same as in previous work.^{6,7} We therefore refrain from repeating any details here.

EXPERIMENTAL RESULTS

The solubility of carbon dioxide (component 3) in solvent mixtures of water (component 1) and [bmim][CH₃SO₄] (component 2) was determined for three different solvent compositions. The mass fractions w'_2 (mole fractions x'_2) of the ionic liquid in the (gas-free) solvent were 0.1501 (0.01255), 0.4956 (0.06604), and 0.8705 (0.3260), respectively. In the isothermal experimental series, the temperature T was about (293, 333, and 373) K. The total pressure p ranged up to about 10 MPa. The experimental data are reported in Tables 2 to 4 as the total pressure that is required to dissolve the given amount of substance (the number of moles) of carbon dioxide in one kilogram of the solvent mixture of (water + [bmim][CH₃SO₄]) (= the molality of carbon dioxide m_3) at a fixed temperature. The molality of CO₂ was at maximum about 1.64 $\text{mol} \cdot \text{kg}^{-1}$, corresponding to a maximum mole fraction of CO₂ in the ternary liquid mixture of about 0.033. The experimental uncertainties are

Table 4. Experimental Results for the Solubility of Carbon Dioxide (3) in Water (1) + [bmim][CH₃SO₄] (2) at $w'_2 = 0.8705 \pm 0.0006$ ($x'_2 = 0.3260 \pm 0.0012$) ($\Delta T = \pm 0.1$ K)^a

T	m_3	p	V/\bar{m}_s
K	mol·kg ⁻¹	MPa	cm ³ ·kg ⁻¹
293.1	0.3800 ± 0.0015	1.027 ± 0.021	858.9 ± 2.6
	0.5824 ± 0.0020	1.582 ± 0.023	864.6 ± 2.6
	0.8365 ± 0.0027	2.303 ± 0.025	872.6 ± 2.7
	1.0705 ± 0.0034	2.928 ± 0.034	883.1 ± 2.7
	1.3528 ± 0.0045	3.712 ± 0.037	891.8 ± 2.7
	1.6373 ± 0.0053	4.484 ± 0.039	901.3 ± 2.8
333.3	0.2361 ± 0.0011	1.210 ± 0.023	874.2 ± 2.7
	0.4806 ± 0.0017	2.405 ± 0.026	885.4 ± 2.7
	0.6992 ± 0.0023	3.606 ± 0.036	891.8 ± 2.7
	0.9236 ± 0.0031	4.822 ± 0.041	899.7 ± 2.7
	1.1612 ± 0.0038	6.242 ± 0.044	911.4 ± 2.8
	1.4149 ± 0.0046	7.783 ± 0.048	918.8 ± 2.8
373.2	1.6146 ± 0.0052	8.962 ± 0.051	925.5 ± 2.8
	0.1928 ± 0.0009	1.488 ± 0.025	895.3 ± 2.7
	0.4075 ± 0.0014	3.082 ± 0.036	903.3 ± 2.8
	0.6300 ± 0.0021	4.839 ± 0.040	911.6 ± 2.8
	0.7809 ± 0.0025	6.117 ± 0.044	918.3 ± 2.8
	0.9512 ± 0.0032	7.539 ± 0.049	927.1 ± 2.8
	1.1267 ± 0.0037	9.091 ± 0.052	930.6 ± 2.9

^a See the footnote in Table 2.

also given in those tables. They were estimated as described previously.^{6,7}

In Figure 1, the experimental results for the total pressure are plotted versus the gas molality at constant temperature and solvent mixture composition. Within the temperature and pressure regions investigated in this study, the total pressure monotonously increases with increasing gas molality at given temperature for all mixtures investigated. Both pure liquids (water and [bmim][CH₃SO₄]) are rather poor solvents for carbon dioxide, while carbon dioxide is better soluble in [bmim][CH₃SO₄] than in water. Therefore, we expected that the pressure that is required to dissolve a certain specified amount of CO₂ in 1 kg of solvent at a constant temperature decreases with increasing mass fraction of the ionic liquid in the solvent. That expectation is met only at the highest investigated temperature (i.e., 373 K), but it fails at (333 and 293) K (see Figure 2). For example, the solubility pressure for dissolving 0.5 mol of CO₂ in 1 kg of solvent at 333 K is about 3.6 MPa in pure water (i.e., $w'_2 = 0$)¹¹ as well as in an aqueous solution at $w'_2 = 0.15$. It decreases only for higher mass fractions of the ionic liquid (for example, to about 3.45 MPa at $w'_2 = 0.5$, to about 2.5 MPa at $w'_2 = 0.87$, and to about 1.8 MPa in pure [bmim][CH₃SO₄]¹²). At 293 K, the solubility pressure even increases from about 1.4 MPa (in pure water) to 1.6 MPa in an aqueous solution at $w'_2 = 0.15$ and to 2.0 MPa at $w'_2 = 0.5$, before it decreases to 1.35 MPa at $w'_2 = 0.87$ to finally reach 0.9 MPa in pure [bmim][CH₃SO₄]. The influence of temperature (at constant solvent composition) is also large, and as expected, the solubility decreases with increasing temperature. For example, the pressure that is required to dissolve 0.5 mol of CO₂ in 1 kg of solvent in a solvent mixture with about 50 mass % of water increases from about 2 MPa at

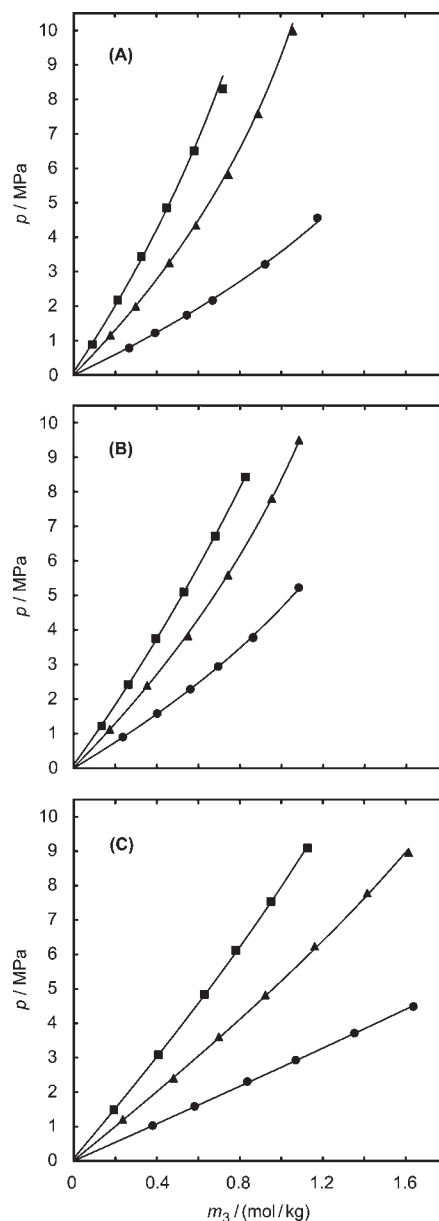


Figure 1. Total pressure (p) above solutions of H₂O (1) + [bmim][CH₃SO₄] (2) + CO₂ (3) versus molality of CO₂ (m_3) in that solution: (A) gas-free mass fraction of the ionic liquid $w'_2 = 0.1501$ (gas-free mole fraction $x'_2 = 0.01255$), (B) $w'_2 = 0.4956$ ($x'_2 = 0.06604$), (C) $w'_2 = 0.8705$ ($x'_2 = 0.3260$); (●, ≈293 K; ▲, ≈333 K; ■, ≈373 K), experimental results; solid line, correlation.

293 K to about 3.5 MPa at 333 K to about 4.8 MPa at 373 K (cf. Figure 1B).

Correlation of Gas Solubility Data. The correlation of the solubility of a single gas in a solvent mixture requires a model for the Gibbs excess energy of the ternary liquid mixture. A particular, thermodynamically rigorous model was developed by Pérez-Salado Kamps³ and successfully applied to correlate the solubility of CO₂ in aqueous solutions of methanol³ and of acetone.¹³ It is therefore also applied here. For better understanding, the model basics are briefly repeated here.

Applying the phase equilibrium conditions requires reference states for the chemical potential for each component. The reference

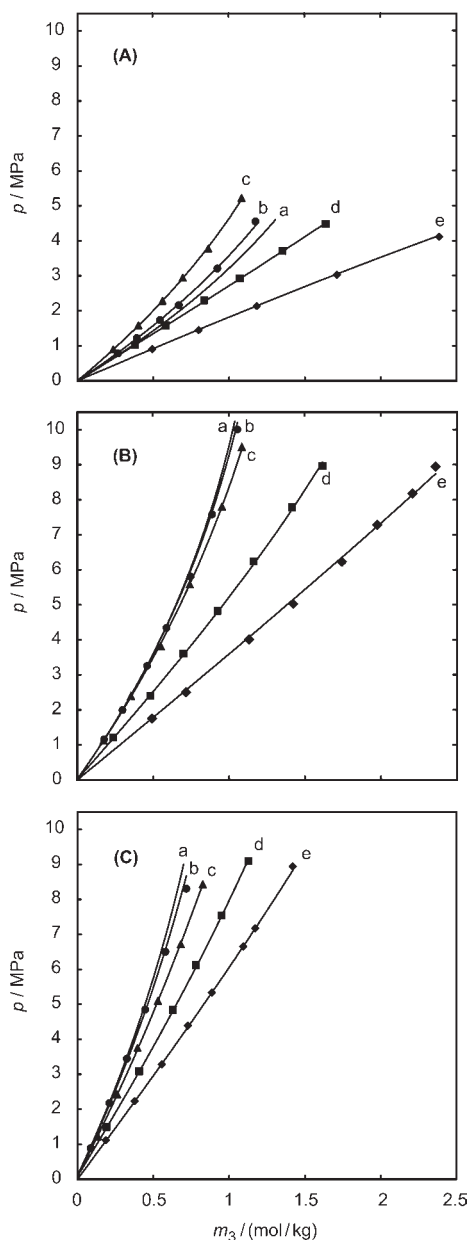


Figure 2. Total pressure (p) above solutions of H_2O (1) + $[\text{bmim}][\text{CH}_3\text{SO}_4]$ (2) + CO_2 (3) versus molality of CO_2 (m_3) in that solution at $T \approx 293$ K (A), 333 K (B), and 373 K (C): (a) pure water solvent ($w'_2 = 0$), correlation by Rumpf and Maurer,¹¹ (b) $w'_2 = 0.1501$ (experimental results and correlation from the present work), (c) $w'_2 = 0.4956$ (experimental results and correlation from the present work), (d) $w'_2 = 0.8705$ (experimental results and correlation from the present work); (e) pure ionic liquid solvent ($w'_2 = 1$) (experimental results from Kumelan et al.,¹² correlation from the present work).

state for the chemical potential of a solvent component (i.e., water (= component 1) and $[\text{bmim}][\text{CH}_3\text{SO}_4]$ (= component 2)) is chosen to be the pure liquid at temperature and pressure of the ternary mixture. For the solute component carbon dioxide (= component 3), the reference state is chosen to be a virtual one molal solution of CO_2 in the liquid solvent mixture of water + $[\text{bmim}][\text{CH}_3\text{SO}_4]$ of fixed composition at the temperature and pressure of the ternary mixture, where CO_2 experiences the same interactions as at infinite dilution in that particular solvent mixture.

The phase equilibrium condition then results in the extended Raoult's law for both solvent components and in the extended Henry's law for the solute. However, following the assumption that the amount of the ionic liquid $[\text{bmim}][\text{CH}_3\text{SO}_4]$ in the vapor phase is negligible (cf. ref 12), the extended Raoult's law is only applied to water here:

$$p_1^{\text{sat}} \phi_1^{\text{sat}} \exp\left[\frac{v_1(p - p_1^{\text{sat}})}{RT}\right] a_1 = f_1 = y_1 p \phi_1 \quad (1)$$

p_1^{sat} , ϕ_1^{sat} , and v_1 are the vapor pressure, the fugacity coefficient of the saturated vapor, and the molar liquid volume of pure water at temperature T , respectively. R and p are the universal gas constant and the total pressure, respectively. a_i is the activity of component i in the liquid phase, f_i is the fugacity of component i , and y_i and ϕ_i are the mole fraction and the fugacity coefficient of component i in the vapor phase.

For carbon dioxide, the phase equilibrium condition results in the extended Henry's law:

$$k_{\text{H},3}^{(m)}(T, p, x'_2) a_3 = f_3 = y_3 p \phi_3 \quad (2)$$

where $k_{\text{H},3}^{(m)}(T, p, x'_2)$ is the molality scale-based Henry's law constant of CO_2 in the solvent mixture. It depends on temperature, total pressure, and composition of the gas-free solvent mixture. That composition is expressed through the mole fraction, x'_2 , of solvent component 2 (i.e., $[\text{bmim}][\text{CH}_3\text{SO}_4]$):

$$x'_2 = \frac{n_2}{n_1 + n_2} = 1 - x'_1 \quad (3)$$

n_1 and n_2 are the amounts of substance (the number of moles) of water and $[\text{bmim}][\text{CH}_3\text{SO}_4]$, respectively.

As usual, Henry's constant $k_{\text{H},3}^{(m)}(T, p, x'_2)$ is split into two contributions

$$k_{\text{H},3}^{(m)}(T, p, x'_2) = k_{\text{H},3}^{(m,0)}(T, x'_2) \exp\left[\frac{v_{3,s}^{\infty}(T, x'_2) \cdot (p - p_s^{\text{sat}}(T, x'_2))}{RT}\right] \quad (4)$$

where $k_{\text{H},3}^{(m,0)}(T, x'_2)$ is Henry's constant of CO_2 on the molality scale in the particular solvent mixture at a vanishing amount of the gas in the solvent mixture liquid, that is, at the vapor pressure $p_s^{\text{sat}}(T, x'_2)$ of that solvent mixture, and $v_{3,s}^{\infty}(T, x'_2)$ is the partial molar volume of CO_2 at infinite dilution in the solvent mixture.

The correlation equations by Saul and Wagner¹⁴ were used to calculate the vapor pressure and the molar volume of liquid water. The virial equation of state was used to calculate vapor phase fugacities. The virial equation was truncated after the second virial coefficient. Details on the virial coefficients are given in the Appendix.

The activity of the solute gas CO_2 (3) in liquid solvent of water (1) and $[\text{bmim}][\text{CH}_3\text{SO}_4]$ (2) is required in eq 2. It is expressed as:

$$a_3 = \left(\frac{m_3}{m^\circ}\right) \cdot \gamma_3 \quad (5)$$

where $m^\circ = 1 \text{ mol} \cdot \text{kg}^{-1}$. The activity coefficient of CO_2 is approximated by

$$\ln \gamma_3 = 2 \cdot \left(\frac{m_3}{m^\circ}\right) \cdot \beta_{3,3}^{(0)}(T, x'_2) + 3 \cdot \left(\frac{m_3}{m^\circ}\right)^2 \cdot \mu_{3,3,3}(T, x'_2) \quad (6)$$

which is a modification of Pitzer's expression for the Gibbs excess energy of electrolyte solutions. $\beta_{3,3}^{(0)}(T, x'_2)$ and $\mu_{3,3,3}(T, x'_2)$ describe the effects of binary and ternary interactions between CO₂ molecules in the solvent mixture of water and [bmim][CH₃SO₄]. Both parameters depend on temperature and composition of the solute-free solvent mixture.

The activity of solvent component water is required in eq 1. As discussed by Pérez-Salado Kamps,³ the activity is the sum of five contributions:

$$\ln a_1 = \ln x_1 - x'_2 \left(\frac{M_s^*}{RT} \right) \left(\frac{m_3}{m^\circ} \right) \left(\frac{\partial \Delta_t G_3^{(x)}}{\partial x'_2} \right)_{T,p} + \ln \gamma_{1, \text{UNIQUAC}} + \ln \gamma_{1, \text{Pitzer}} + \ln \gamma_{1, \text{conv}} \quad (7)$$

The first two terms on the right side of the equation describe the dilution from pure water to an ideal liquid mixture where for the solvent components the reference state for the chemical potential is the pure liquid, and for the solute component carbon dioxide the reference state is a virtual pure liquid where CO₂ experiences the same interactions as at infinite dilution in that particular solvent mixture. In that ideal mixture, the composition of the ternary mixture is expressed by the *mole fraction scale*; that is, x_1 is the mole fraction of water in the liquid mixture of (CO₂ + water + [bmim][CH₃SO₄]). In particular, the second contribution accounts for the transfer of the solute from pure water to the solvent mixture. The remaining terms on the right side of eq 7 consider the various deviations from that ideal mixture. The third term corrects the nonideal behavior of the solvent mixture via the universal quasichemical (UNIQUAC) model for the Gibbs excess energy. The final two terms result from the presence of the solute. The fourth contribution results from the nonideal behavior of the solute in the solvent mixture which results—in analogy to eq 6—from binary and ternary interactions between solute molecules. Since that fourth contribution results from the extension to solvent mixtures of Pitzer's expression for the Gibbs excess energy of aqueous electrolyte solutions, it is characterized by subscript "Pitzer". The final contribution accounts for the change that is caused by applying the molality scale to express the amount of the solute in the solvent mixture.

In eq 7, M_s^* is the relative molar mass of the solvent mixture divided by 1000. For the solvent mixture (water + [bmim][CH₃SO₄]), it is

$$M_s^* = M_1^* + x'_2(M_2^* - M_1^*) \quad (8)$$

where $M_1^* = 0.0180153$ (for water) and $M_2^* = 0.2503202$ (for [bmim][CH₃SO₄]). $\Delta_t G_3^{(x)}$ is the molar Gibbs energy of transfer of CO₂ from pure water to the solvent mixture of water and [bmim][CH₃SO₄] based on the *mole fraction scale*. That Gibbs energy of transfer depends on temperature, pressure, and the composition of the (gas-free) solvent mixture. It can be calculated from the molality scale-based Henry's constant of CO₂ in pure water, $k_{H,3}^{(m)}(T, p, x'_2 = 0)$, and in liquid mixtures of (water + [bmim][CH₃SO₄]), $k_{H,3}^{(m)}(T, p, x'_2)$, as follows:

$$\Delta_t G_3^{(x)}(T, p, x'_2) = RT \ln \left(\frac{k_{H,3}^{(m)}(T, p, x'_2)}{k_{H,3}^{(m)}(T, p, x'_2 = 0)} \right) - RT \ln \left(\frac{M_s^*}{M_1^*} \right) \quad (9)$$

where the first term on the right side denotes the *molality scale*-based Gibbs energy of transfer of CO₂ from pure water to the

solvent mixture of water and [bmim][CH₃SO₄]:

$$\Delta_t G_3^{(m)}(T, p, x'_2) = RT \ln \left(\frac{k_{H,3}^{(m)}(T, p, x'_2)}{k_{H,3}^{(m)}(T, p, x'_2 = 0)} \right) \quad (10)$$

The second term on the right side of eq 9 corrects for the change from molality scale to mole fraction scale in the molar Gibbs transfer energy.

The contribution $\ln \gamma_{1, \text{UNIQUAC}}$ depends only on temperature T and the mole fraction of the ionic liquid, x'_2 , but it does not depend on the dissolved amount of gas (cf. ref 3). Numerical values for the UNIQUAC size and surface parameters of water were taken from a previous work³ ($r_1 = 0.92$, $q_1 = 1.4$). For [bmim][CH₃SO₄], they were adopted from Santiago et al.¹⁵ ($r_2 = 8.9208$, $q_2 = 7.09$). There is only very scarce experimental information available on the VLE of the binary system (water + [bmim][CH₃SO₄]) (see, e.g., Calvar et al.¹⁶). The influence of that VLE on the correlation of the solubility of CO₂ in those solutions is marginal. Therefore, we neglect differences in interactions between all molecules in the solvent mixture. Then, the UNIQUAC term reduces to its combinatorial contribution:

$$\ln \gamma_{1, \text{UNIQUAC}} = \ln \left(\frac{\phi'_1}{x'_1} \right) + 1 - \frac{\phi'_1}{x'_1} - \frac{z}{2} \cdot q_1 \cdot \left[\ln \left(\frac{\phi'_1}{\theta'_1} \right) + 1 - \frac{\phi'_1}{\theta'_1} \right] \quad (11)$$

where:

$$\phi'_1 = \frac{x'_1 \cdot r_1}{x'_1 \cdot r_1 + x'_2 \cdot r_2} \quad (12)$$

$$\theta'_1 = \frac{x'_1 \cdot q_1}{x'_1 \cdot q_1 + x'_2 \cdot q_2} \quad (13)$$

The mathematical expression for the contribution of Pitzer's equation to the activity coefficient of water is (cf. also ref 3):

$$\ln \gamma_{1, \text{Pitzer}} = -M_1^* \left[\left(\frac{m_3}{m^\circ} \right)^2 \cdot \beta_{3,3}^{(0)} + 2 \left(\frac{m_3}{m^\circ} \right)^3 \cdot \mu_{3,3,3} \right] - M_s^* \cdot x'_2 \left[\left(\frac{m_3}{m^\circ} \right)^2 \frac{\partial \beta_{3,3}^{(0)}}{\partial x'_2} + \left(\frac{m_3}{m^\circ} \right)^3 \frac{\partial \mu_{3,3,3}}{\partial x'_2} \right] \quad (14)$$

Pitzer's G^E equation is based on the molality scale, whereas the UNIQUAC equation is based on the mole fraction scale. A conversion term $\ln \gamma_{1, \text{conv}}$ is therefore necessary in eq 7 (cf. ref 3):

$$\ln \gamma_{1, \text{conv}} = - \left(\frac{m_3}{m^\circ} \right) \cdot M_s^* + \ln \left[1 + \left(\frac{m_3}{m^\circ} \right) \cdot M_s^* \right] \quad (15)$$

The applied model requires information for Henry's constant $k_{H,3}^{(m,0)}(T, x'_2)$ of CO₂ in liquid mixtures of water + [bmim][CH₃SO₄] at the saturation pressure of that solvent mixture $p_s^{\text{sat}}(T, x'_2)$, the partial molar volume of CO₂ at infinite dilution in that solvent mixture $v_{3,s}^\infty(T, x'_2)$, and finally the parameters $\beta_{3,3}^{(0)}(T, x'_2)$ and $\mu_{3,3,3}(T, x'_2)$ for interactions between CO₂ molecules in the solvent mixture.

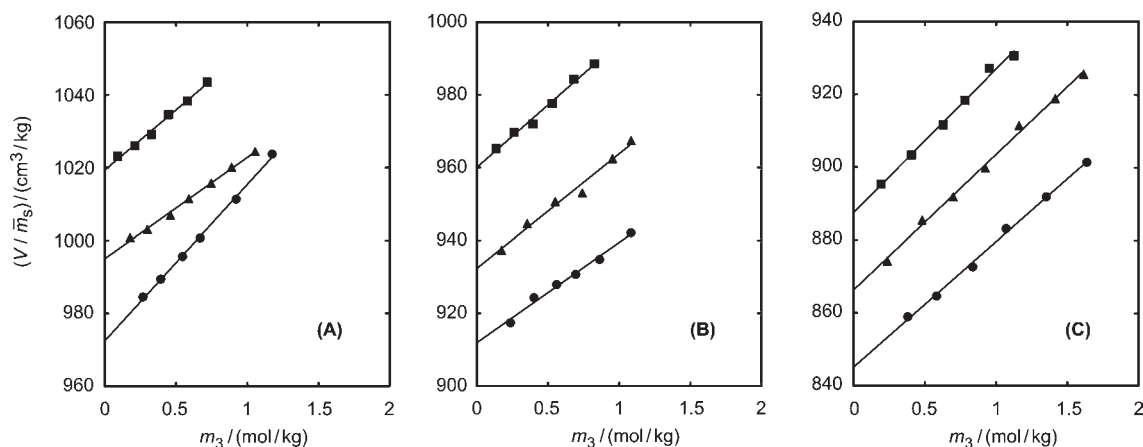


Figure 3. Volume of liquid mixtures of ($\text{H}_2\text{O} + [\text{bmim}][\text{CH}_3\text{SO}_4] + \text{CO}_2$) divided by the mass of solvent components ($\text{H}_2\text{O} + [\text{bmim}][\text{CH}_3\text{SO}_4]$), V/\bar{m}_s , versus molality of CO_2 (m_3) in that liquid mixture: (A) gas-free mass fraction of the ionic liquid $w'_2 = 0.1501$ (gas-free mole fraction $x'_2 = 0.01255$), (B) $w'_2 = 0.4956$ ($x'_2 = 0.06604$), (C) $w'_2 = 0.8705$ ($x'_2 = 0.3260$); (●, ≈ 293 K; ▲, ≈ 333 K; ■, ≈ 373 K), experimental results; solid line, correlation lines.

Table 5. Experimental Results for the Partial Molar Volume of Carbon Dioxide (3) Infinitely Diluted in a Solvent Mixture of H_2O (1) + $[\text{bmim}][\text{CH}_3\text{SO}_4]$ (2), $v_{3,s}^\infty(T, x'_2)$, and for the Specific Volume of the Solvent Mixture, $v_s(T, x'_2)$

T	x'_2	$v_{3,s}^\infty$ $\text{cm}^3 \cdot \text{mol}^{-1}$	method 1 ^a	method 2 ^b
			v_s $\text{cm}^3 \cdot \text{kg}^{-1}$	v_s $\text{cm}^3 \cdot \text{kg}^{-1}$
293.2	0	32.7 ^c	1001.9 ^e	1001.7 ± 0.1
293.1	0.01255	42.9 ± 5.6	972.5 ± 2.8	975.0 ± 0.1
293.2	0.06604	27.6 ± 5.6	911.9 ± 2.8	909.8 ± 0.1
293.1	0.3260	34.4 ± 5.6	845.1 ± 2.8	843.9 ± 0.1
293.2	1	37.1 ^d	824.2 ^f	825.3 ± 0.1
333.2	0	34.7 ^c	1017.1 ^e	
333.1	0.01255	27.8 ± 5.6	995.0 ± 2.8	
333.2	0.06604	31.5 ± 5.6	932.3 ± 2.8	
333.3	0.3260	37.2 ± 5.6	866.3 ± 2.8	
333.1	1	37.3 ^d	842.5 ^f	
373.1	0	38.3 ^c	1043.4 ^e	
373.1	0.01255	33.1 ± 5.6	1019.4 ± 2.8	
373.1	0.06604	34.3 ± 5.6	960.0 ± 2.8	
373.2	0.3260	39.4 ± 5.6	887.5 ± 2.8	
373.1	1	37.6 ^d	860.3 ^f	

^a From an extrapolation of the volumetric data of the present work.

^b From direct density measurements of the present work. ^c From method by Brelvi and O'Connell.¹⁸ ^d From Kumelan et al.¹⁷ (eq 18). ^e From Saul and Wagner.¹⁴ ^f From Kumelan et al.¹⁷

$p_s^{\text{sat}}(T, x'_2)$ was calculated by applying eq 1 for the gas-free solvent mixture of (water + $[\text{bmim}][\text{CH}_3\text{SO}_4]$). All other missing properties and parameters were deduced from the experimental results reported in Tables 2 to 4. $v_{3,s}^\infty(T, x'_2)$ was determined from the experimental results for V/\bar{m}_s (cf., ref 17), which is the ratio of the volume of the liquid mixture of ($\text{CO}_2 + \text{H}_2\text{O} + [\text{bmim}][\text{CH}_3\text{SO}_4]$) and the mass of the solvent mixture of ($\text{H}_2\text{O} + [\text{bmim}][\text{CH}_3\text{SO}_4]$) in the view cell. The ratio is plotted versus the molality of CO_2 at constant temperature T and

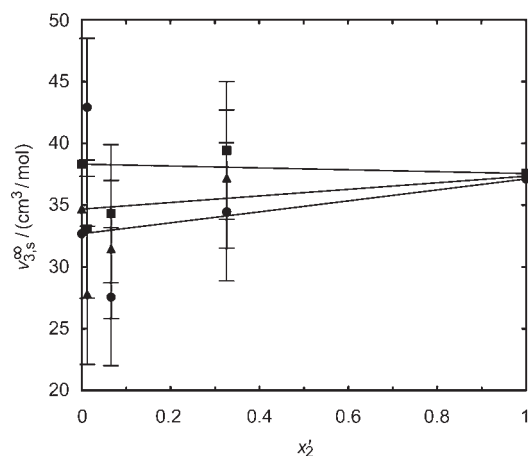


Figure 4. Partial molar volume of CO_2 (3) at infinite dilution in a solvent mixture of H_2O (1) + $[\text{bmim}][\text{CH}_3\text{SO}_4]$ (2), $v_{3,s}^\infty(T, x'_2)$, plotted versus the gas-free mole fraction of $[\text{bmim}][\text{CH}_3\text{SO}_4]$ in the liquid, x'_2 , at a constant temperature T : (●, ≈ 293 K; ▲, ≈ 333 K; ■, ≈ 373 K), experimental results; solid line, correlation according to eq 17.

solvent mixture composition x'_2 in Figure 3. The slope of that curve (in principle at $m_3 \rightarrow 0$) corresponds to the partial molar volume of CO_2 in the liquid mixture at infinite dilution.¹⁷ Figure 3 shows that the experimental results for V/\bar{m}_s reveal (within experimental uncertainty) a linear dependency from the molality of CO_2 . Therefore, the partial molar volume of CO_2 at infinite dilution of that gas in the solvent mixture of ($\text{H}_2\text{O} + [\text{bmim}][\text{CH}_3\text{SO}_4]$) is determined from that slope:

$$v_{3,s}^\infty(T, x'_2) = \left(\frac{\partial V}{\partial n_3} \right)_{T, p, n_1, n_2} = \left(\frac{\partial (V/\bar{m}_s)}{\partial m_3} \right)_{T, x'_2} \quad (16)$$

where n_i is the amount of substance (the number of moles) of component i . The interception of that straight line with the ordinate gives the specific volume $v_s(T, x'_2)$ of the solvent mixture of ($\text{H}_2\text{O} + [\text{bmim}][\text{CH}_3\text{SO}_4]$) at (T, x'_2) which is, however, not required for the present gas solubility correlation. The reciprocal of $v_s(T, x'_2)$ is the density $\rho_s(T, x'_2)$ of the solvent mixture.

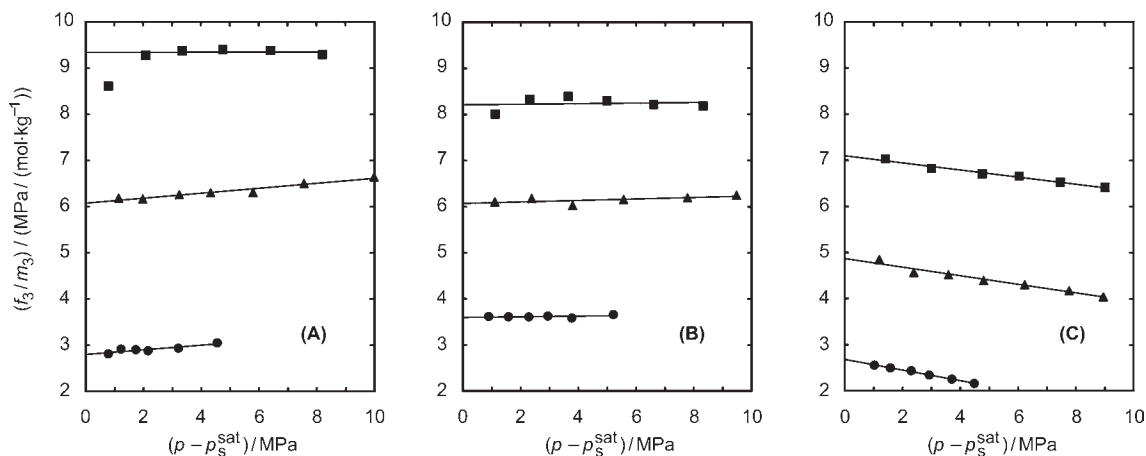


Figure 5. Influence of $p - p_s^{\text{sat}}$ (p = total pressure, p_s^{sat} = vapor pressure of the solvent ($\text{H}_2\text{O} + [\text{bmim}][\text{CH}_3\text{SO}_4]$)) on the ratio of the fugacity of CO_2 to the molality of CO_2 (in the liquid): (A) gas-free mass fraction of the ionic liquid $w'_2 = 0.1501$ (gas-free mole fraction $x'_2 = 0.01255$), (B) $w'_2 = 0.4956$ ($x'_2 = 0.06604$), (C) $w'_2 = 0.8705$ ($x'_2 = 0.3260$); (●, ≈ 293 K; ▲, ≈ 333 K; ■, ≈ 373 K), experimental results; solid line, extrapolation lines.

The numerical values for $v_{3,s}^{\infty}(T, x'_2)$ and $v_s(T, x'_2)$ resulting from those plots are given in Table 5 together with their estimated experimental uncertainties. The numerical values for $v_{3,s}^{\infty}(T, x'_2)$ in the solvent mixture range from about $(28 \text{ to } 43) \text{ cm}^3 \cdot \text{mol}^{-1}$; that is, they are close to the numerical values for the partial molar volume of CO_2 in the pure solvents (cf. Table 5). The uncertainty of $v_{3,s}^{\infty}(T, x'_2)$ was estimated from randomly excluding a single experimental data point for V/\bar{m}_s from the evaluation as well as randomly shifting some experimental data points (for V/\bar{m}_s) to their lower/upper experimental uncertainty limits (cf. ref 17). The uncertainty of $v_{3,s}^{\infty}(T, x'_2)$ is about $5.6 \text{ cm}^3 \cdot \text{mol}^{-1}$; that is, the relative uncertainty amounts to about 15 %. For 293 K, the experimental results for $v_s(T, x'_2)$ resulting from the extrapolation of the volumetric data V/\bar{m}_s can be directly compared to the results from the independent density measurements. As shown in Table 5, the deviations between both values fall within the estimated uncertainty of the extrapolation results.

The numerical values for $v_{3,s}^{\infty}(T, x'_2)$ are plotted versus x'_2 in Figure 4. Because (a) the influence of $v_{3,s}^{\infty}(T, x'_2)$ on the calculation results for the solubility of CO_2 in the solvent mixtures is small, (b) the relative uncertainty of the experimental results for $v_{3,s}^{\infty}(T, x'_2)$ amounts to about 15 %, and (c) the experimental results reveal some scattering, the influence of the composition of the solvent mixture (i.e., the influence of x'_2) on $v_{3,s}^{\infty}(T, x'_2)$ was approximated by the simplest relation which is properly applicable:

$$v_{3,s}^{\infty}(T, x'_2) = (1 - x'_2) \cdot v_{3,s}^{\infty}(T, x'_2 = 0) + x'_2 \cdot v_{3,s}^{\infty}(T, x'_2 = 1) \quad (17)$$

The partial molar volume of CO_2 infinitely diluted in water, $v_{3,s}^{\infty}(T, x'_2 = 0)$, was calculated using the method of Brelvi and O'Connell¹⁸ (for some details, see Appendix). The partial molar volume of CO_2 infinitely diluted in $[\text{bmim}][\text{CH}_3\text{SO}_4]$, $v_{3,s}^{\infty}(T, x'_2 = 1)$, was adopted from Kumelan et al.¹⁷

$$v_{3,s}^{\infty}(T, x'_2 = 1) / (\text{cm}^3 \cdot \text{mol}^{-1}) = 35.5 + 0.0055(T/\text{K}) \quad (18)$$

In the next step, Henry's constant on the molality scale, $k_{\text{H},3}^{(m,0)}(T, x'_2)$, was determined by executing the commonly used

extrapolation procedure (at constant temperature T and solvent mixture composition x'_2):

$$\ln k_{\text{H},3}^{(m,0)}(T, x'_2) = \lim_{p \rightarrow p_s^{\text{sat}}(T, x'_2)} \ln \left[\frac{f_3(T, p, y_j)}{(m_3/m^\circ)} \right] \quad (19)$$

where f_3 is the fugacity of CO_2 at equilibrium temperature, pressure, and vapor-phase composition (cf. eq 2).

$$f_3(T, p, y_j) = y_3 \cdot p \cdot \phi_3(T, p, y_j) \quad (20)$$

The vapor-phase composition was not determined experimentally. Therefore, for every individual experimental data point (T , x'_2 , m_3 , and p), the vapor phase composition was estimated iteratively employing eqs 1, 7, 11, and 15 (see ref 3). In that estimation, both $\Delta_r G_3^{(x)}$ and $\ln \gamma_{1,\text{Pitzer}}$ were set to zero. Calculation results for $\ln[f_3/(m_3/m^\circ)]$ are plotted in Figure 5 versus the difference between the total pressure p above the ternary mixture ($\text{CO}_2 + \text{water} + [\text{bmim}][\text{CH}_3\text{SO}_4]$) and the vapor pressure $p_s^{\text{sat}}(T, x'_2)$ of the gas-free liquid mixture (water + $[\text{bmim}][\text{CH}_3\text{SO}_4]$).

The numerical values for $k_{\text{H},3}^{(m,0)}(T, x'_2)$ resulting from these extrapolations are given in Table 6 together with their estimated uncertainties. The uncertainty was estimated as the standard deviation from the extrapolation line which was determined from a linear regression. Henry's constant is often reported on a mole fraction scale basis. Henry's constant on a mole fraction scale $k_{\text{H},3}^{(x,0)}(T, x'_2)$ is related to Henry's constant on the molality scale $k_{\text{H},3}^{(m,0)}(T, x'_2)$ by:

$$k_{\text{H},3}^{(x,0)}(T, x'_2) = \frac{k_{\text{H},3}^{(m,0)}(T, x'_2)}{M_s^*} \quad (21)$$

where M_s^* is the relative molar mass of the gas-free solvent mixture divided by 1000 (cf. eq 8). The results for $k_{\text{H},3}^{(x,0)}(T, x'_2)$ are also given in Table 6. Numerical values for $\ln(k_{\text{H},3}^{(m,0)}(T, x'_2)/\text{MPa})$ are plotted versus x'_2 in Figure 6.

At 293 K, Henry's constant runs through a distinguished maximum when the mole fraction of the ionic liquid in the solvent mixture changes from 0 to 1. With increasing temperature, the composition of the solvent mixture at that maximum is shifted to lower mole fractions of the ionic liquid and the

Table 6. Experimental Results for Henry's Constant of Carbon Dioxide (3) in Solvent Mixtures of H₂O (1) + [bmim][CH₃SO₄] (2)

T		Henry's constant	
		on molality scale	on mole fraction scale
		$k_{H,3}^{(m,0)}$	$k_{H,3}^{(x,0)}$
K	x'_2	MPa	MPa
293.2	0	2.606 ^a	144.6
293.1	0.01255	2.800 ± 0.034	133.8 ± 1.6
293.2	0.06604	3.597 ± 0.022	107.8 ± 0.7
293.1	0.3260	2.681 ± 0.010	28.60 ± 0.11
293.2	1	1.866 ^b	7.455
333.2	0	6.038 ^a	335.2
333.1	0.01255	6.075 ± 0.041	290.3 ± 2.0
333.2	0.06604	6.068 ± 0.058	181.9 ± 1.7
333.3	0.3260	4.867 ± 0.052	51.91 ± 0.56
333.1	1	3.553 ^b	14.20
373.1	0	9.119 ^a	506.2
373.1	0.01255	9.338 ± 0.057	446.2 ± 2.7
373.1	0.06604	8.208 ± 0.133	246.1 ± 4.0
373.2	0.3260	7.098 ± 0.031	75.70 ± 0.33
373.1	1	5.800 ^b	23.17

^aRumpf and Maurer¹¹ (eq 23). ^bKumelán et al.¹² (eq 24).

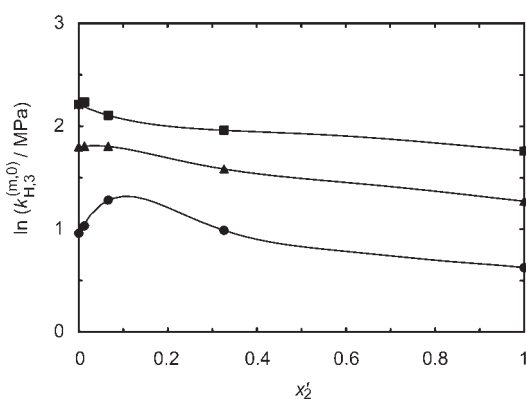


Figure 6. Henry's constant (on molality scale) of CO₂ (3) in a solvent mixture of (H₂O (1) + [bmim][CH₃SO₄] (2)), $\ln(k_{H,3}^{(m,0)}(T, x'_2)/\text{MPa})$, plotted versus the gas-free mole fraction of [bmim][CH₃SO₄] in the liquid, x'_2 , at a constant temperature T : (●, ≈ 293 K; ▲, ≈ 333 K; ■, ≈ 373 K), experimental results; solid line, correlation according to eq 22.

difference between the maximum in $\ln(k_{H,3}^{(m,0)}(T, x'_2))$, and a straight line that links the corresponding data points for the solubility of CO₂ in the pure solvents decreases. Figure 6 shows that the influence of solvent composition on Henry's constant of CO₂ is rather complicated, and therefore a large number of parameters is required for a correlation. Interestingly, the same phenomenon was recently observed during similar measurements of the ternary system (CO₂ + water + quaternary carboxylate ionic liquid) at 293 K.²⁰

The influence of the composition of the solvent mixture on Henry's law constant $k_{H,3}^{(m,0)}(T, x'_2)$ was approximated by a

Table 7. Redlich–Kister Parameters in Equations 22, 25, and 26

$k_{H,3}^{(m,0)}$	$A_{n,j}$	$j = 1$	$j = 2$	$j = 3$
$n = 0$		5.9481	-4520	826720
$n = 1$		5.0817	-4688.3	971560
$n = 2$		2.0984	-3662.1	1006900
$n = 3$		33.001	-25583	4933600
$n = 4$		34.9474	-26603	5050200
$n = 5$		-3.079	1017.9	30300
$\beta_{3,3}^{(0)}$	$B_{n,j}$	$j = 1$	$j = 2$	$j = 3$
$n = 0$		0.16772	-382.68	74571
$\mu_{3,3,3}$	$C_{n,j}$	$j = 1$	$j = 2$	$j = 3$
$n = 3$		13.1666	-7764.1	1146330
$n = 5$		-39.2343	23142.8	-3424390

Redlich–Kister type of approach:

$$\begin{aligned} \ln[k_{H,3}^{(m,0)}(T, x'_2)/\text{MPa}] &= (1 - x'_2) \ln[k_{H,3}^{(m,0)}(T, x'_2 = 0)/\text{MPa}] \\ &+ x'_2 \ln[k_{H,3}^{(m,0)}(T, x'_2 = 1)/\text{MPa}] \\ &+ (1 - x'_2) \cdot x'_2 \cdot \sum_{n=0}^5 \left[A_{n,1} + \frac{A_{n,2}}{T/\text{K}} + \frac{A_{n,3}}{(T/\text{K})^2} \right] (1 - 2x'_2)^n \end{aligned} \quad (22)$$

where $k_{H,3}^{(m,0)}(T, x'_2 = 0)$ and $k_{H,3}^{(m,0)}(T, x'_2 = 1)$ are the molality scale-based Henry's law constants of CO₂ in water and in [bmim][CH₃SO₄], respectively, and $A_{n,j}$ (for $n = 0$ to 5 and $j = 1$ to 3) are Redlich–Kister parameters.¹⁹ Henry's law constants were taken from Rumpf and Maurer¹¹

$$\begin{aligned} \ln[k_{H,3}^{(m,0)}(T, x'_2 = 0)/\text{MPa}] &= 192.876 - \frac{9624.41}{(T/\text{K})} \\ &- 28.7488 \ln(T/\text{K}) + 0.0144074(T/\text{K}) \end{aligned} \quad (23)$$

and from Kumelán et al.,¹² respectively:

$$\begin{aligned} \ln[k_{H,3}^{(m,0)}(T, x'_2 = 1)/\text{MPa}] \\ = 7.2738 - \frac{1775}{(T/\text{K})} - 0.002033(T/\text{K}) \end{aligned} \quad (24)$$

The Redlich–Kister parameters $A_{n,j}$ were adjusted following two criteria, namely, to match as good as possible the numerical values from Table 6 by as well attaining a more or less reasonable curve progression within the gas-free ionic liquid mole fraction range $0.326 < x'_2 < 1$ which is not covered by experimental gas solubility data. The resulting parameters are listed in Table 7. The number of Redlich–Kister parameters seems to be quite large, and it should be mentioned that this approach is not applicable to predict Henry's law constants at solvent compositions $0.326 < x'_2 < 1$. But for the purpose of the present work, that number of Redlich–Kister parameters was required, and the correlation agrees with the experimental results for Henry's law constants within the estimated experimental uncertainty. The correlation results are also shown in Figure 6.

Pitzer parameters $\beta_{3,3}^{(0)}(T, x'_2)$ and $\mu_{3,3,3}(T, x'_2)$ were then determined as follows: For each experimental series (T, x'_2) = const, this pair of parameters was treated as adjustable parameters,

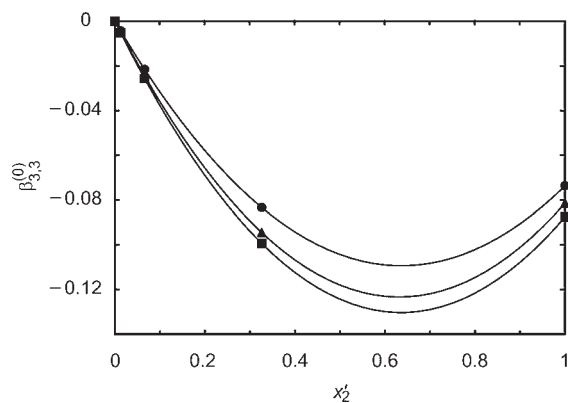


Figure 7. Pitzer parameter for binary interactions between CO₂ (3) molecules in a solvent mixture of H₂O (1) + [bmim][CH₃SO₄] (2), $\beta_{3,3}^{(0)}(T, x'_2)$, plotted versus the gas-free mole fraction of [bmim][CH₃SO₄] in the liquid, x'_2 , at a constant temperature T : (●, ≈ 293 K; ▲, ≈ 333 K; ■, ≈ 373 K) data determined from experimental gas solubility data at $x'_2 = \text{const.}$ and $T = \text{const.}$ (for details, see text); solid line, correlation curve according to eq 25.

and the sum of squared residuals for the total pressure was minimized—a residual being the difference between an experimental value and the value provided by the model. The resulting pair of parameters is plotted in Figures 7 and 8 versus x'_2 . They were correlated as:

$$\beta_{3,3}^{(0)}(T, x'_2) = (1 - x'_2) \cdot \beta_{3,3}^{(0)}(T, x'_2 = 0) + x'_2 \cdot \beta_{3,3}^{(0)}(T, x'_2 = 1) + (1 - x'_2) \cdot x'_2 \left[B_{0,1} + \frac{B_{0,2}}{T/K} + \frac{B_{0,3}}{(T/K)^2} \right] \quad (25)$$

$$\mu_{3,3,3}(T, x'_2) = (1 - x'_2) \cdot \mu_{3,3,3}(T, x'_2 = 0) + x'_2 \cdot \mu_{3,3,3}(T, x'_2 = 1) + (1 - x'_2) \cdot x'_2 \left\{ \left[C_{3,1} + \frac{C_{3,2}}{T/K} + \frac{C_{3,3}}{(T/K)^2} \right] (1 - 2x'_2)^3 + \left[C_{5,1} + \frac{C_{5,2}}{T/K} + \frac{C_{5,3}}{(T/K)^2} \right] (1 - 2x'_2)^5 \right\} \quad (26)$$

The Pitzer parameters for interactions between CO₂ molecules in pure water were adopted from Rumpf and Maurer:¹¹

$$\beta_{3,3}^{(0)}(T, x'_2 = 0) = 0 \quad (27)$$

$$\mu_{3,3,3}(T, x'_2 = 0) = 0 \quad (28)$$

The Pitzer parameters for interactions between CO₂ molecules in pure [bmim][CH₃SO₄] were adopted from Kumeljan et al.¹⁷ $\beta_{3,3}^{(0)}(T, x'_2 = 1) = -0.1121 + 8.636/(T/K)$, $\mu_{3,3,3}(T, x'_2 = 1) = 0$. (Note that there is an incorrect sign in ref 17.) However, Kumeljan et al.¹⁷ did not use the virial equation of state for pure CO₂ in their correlation but the equation by Span and Wagner.⁹ Therefore, a fine-tuning was accomplished here which resulted in:

$$\beta_{3,3}^{(0)}(T, x'_2 = 1) = -0.1386 + \frac{19.04}{T/K} \quad (29)$$

$$\mu_{3,3,3}(T, x'_2 = 1) = 0 \quad (30)$$

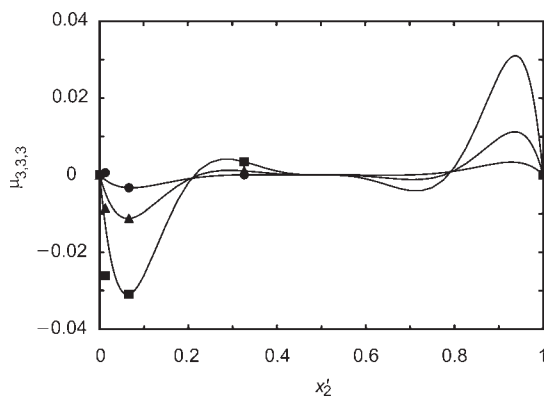


Figure 8. Pitzer parameter for ternary interactions between CO₂ (3) molecules in a solvent mixture of H₂O (1) + [bmim][CH₃SO₄] (2), $\mu_{3,3,3}(T, x'_2)$, plotted versus the gas-free mole fraction of [bmim][CH₃SO₄] in the liquid, x'_2 , at a constant temperature T : (●, ≈ 293 K; ▲, ≈ 333 K; ■, ≈ 373 K) data determined from experimental gas solubility data at $x'_2 = \text{const.}$ and $T = \text{const.}$ (for details, see text); solid line, correlation curve according to eq 26.

The Redlich–Kister parameters¹⁹ in eqs 25 and 26 ($B_{0,j}$ and $C_{n,j}$ for $n = 3, 5$ and $j = 1$ to 3) are listed in Table 7. It has to be mentioned again, that the mole fraction range $0.326 < x'_2 < 1$ was not covered by our experiments.

The approach achieves a very satisfactory agreement between correlated and experimental data for the total pressure above liquid mixtures of (CO₂ + water + [bmim][CH₃SO₄]) with average relative and absolute deviations amounting to only 1.05 % and 0.043 MPa, respectively (see Figure 1).

Thermodynamic Properties of Solution/Transfer. Thermodynamic properties of solution of CO₂ in mixtures of (water + [bmim][CH₃SO₄]) (on the molality scale) are calculated from the correlation of Henry's constant given above applying well-known thermodynamic relations (cf., for example, ref 3):

$$\Delta_{\text{sol}}G_3^{(m)}(T, p, x'_2) = RT \ln[k_{\text{H},3}^{(m)}(T, p, x'_2)/p^\circ] \quad (31)$$

$$\Delta_{\text{sol}}H_3^{(m)}(T, p, x'_2) = R \left(\frac{\partial \ln[k_{\text{H},3}^{(m)}(T, p, x'_2)/p^\circ]}{\partial(1/T)} \right)_{p, x'_2} \quad (32)$$

$$\Delta_{\text{sol}}S_3^{(m)} = (\Delta_{\text{sol}}H_3^{(m)} - \Delta_{\text{sol}}G_3^{(m)})/T \quad (33)$$

Numerical values for $\Delta_{\text{sol}}G_3^{(m)}$, $\Delta_{\text{sol}}H_3^{(m)}$, and $\Delta_{\text{sol}}S_3^{(m)}$ resulting from those equations at standard temperature and pressure ($T^\circ = 298.15$ K, $p^\circ = 0.1$ MPa) and at the experimental solvent mixture compositions (x'_2), and additionally for $x'_2 = 0$ and 1, are given in Table 8.

Thermodynamic properties of transfer of CO₂ from pure water to mixtures of water + [bmim][CH₃SO₄] (on the molality scale) are calculated from the correlation of Henry's constant given above (cf., ref 3):

$$\Delta_t G_3^{(m)}(T, p, x'_2) = RT \ln \left[\frac{k_{\text{H},3}^{(m)}(T, p, x'_2)}{k_{\text{H},3}^{(m)}(T, p, x'_2 = 0)} \right] \quad (34)$$

Table 8. Standard State ($T^\circ = 298.15$ K, $p^\circ = 0.1$ MPa) Thermodynamic Properties of Solution of CO₂ (3) in Water + [bmim][CH₃SO₄] (On the Molality Scale)

x'_2	$\Delta_{\text{sol}}G_3^{\circ(m)}$	$\Delta_{\text{sol}}H_3^{\circ(m)}$	$\Delta_{\text{sol}}S_3^{\circ(m)}$
	kJ·mol ⁻¹	kJ·mol ⁻¹	J·mol ⁻¹ ·K ⁻¹
0	8.420	-19.39	-93.3
0.01255	8.618	-17.22	-86.7
0.06604	9.081	-11.51	-69.1
0.3260	8.376	-12.89	-71.3
1	7.482	-13.25	-69.5

Table 9. Standard State ($T^\circ = 298.15$ K, $p^\circ = 0.1$ MPa) Thermodynamic Properties of Transfer of CO₂ (3) from Pure Water to Water + [bmim][CH₃SO₄] (On the Molality Scale)

x'_2	$\Delta_t G_3^{\circ(m)}$	$\Delta_t H_3^{\circ(m)}$	$\Delta_t S_3^{\circ(m)}$
	kJ·mol ⁻¹	kJ·mol ⁻¹	J·mol ⁻¹ ·K ⁻¹
0.01255	0.198	2.172	6.6
0.06604	0.661	7.882	24.2
0.3260	-0.044	6.506	22.0
1	-0.938	6.143	23.7

$$\Delta_t H_3^{\circ(m)}(T, p, x'_2) = R \left(\frac{\partial \ln \left[\frac{k_{H,3}^{(0)}(T, p, x'_2)}{k_{H,3}^{(0)}(T, p, x'_2 = 0)} \right]}{\partial(1/T)} \right)_{p, x'_2} \quad (35)$$

$$\Delta_t S_3^{\circ(m)} = (\Delta_t H_3^{\circ(m)} - \Delta_t G_3^{\circ(m)})/T \quad (36)$$

Numerical values for $\Delta_t G_3^{\circ(m)}$, $\Delta_t H_3^{\circ(m)}$, and $\Delta_t S_3^{\circ(m)}$ at standard temperature and pressure and at the experimental solvent mixture compositions (x'_2) as well as for $x'_2 = 1$, resulting from those equations (or directly from the data given in Table 8), are given in Table 9.

CONCLUSIONS

A sound base of experimental data is required to develop correlation and prediction methods for the solubility of gases in solvent mixtures: This statement also holds for solvent mixtures where at least one of the solvent components is an ionic liquid. The present work reports experimental results for the solubility of CO₂ in solvent mixtures of water and the ionic liquid [bmim][CH₃SO₄]. The experimental data cover a wide range of solvent mixture composition, as well as wide ranges in temperature and pressure. The new experimental data are reproduced almost within experimental uncertainty by means of a thermodynamic model which applies an unsymmetrical normalization of the chemical potentials in an extension to solvent mixtures of the conventional Pitzer's molality scale-based equation for the Gibbs excess energy. In a forthcoming publication, both the experimental investigations and the correlation

Table A1

component	i	a_i	b_i	c_i	d_i	T/K
H ₂ O	1	-53.527	-39.287	647.3	4.277	373–577
CO ₂	3	65.703	-184.854	304.16	1.36	273–573

Table A2

component	i	$T_{c,i}$	$p_{c,i}$	μ_i	$R_{D,i}$
		K	MPa	10 ⁻³⁰ Cm	10 ⁻¹⁰ m
H ₂ O	1	647.3	22.13	6.10	0.615
CO ₂	3	241.0	5.38	0	0.9918
η_{ij}		H ₂ O		CO ₂	
H ₂ O		1.7		0.3	
CO ₂		0.3		0.16	

Table A3

T	$B_{1,3}$
K	cm ³ ·mol ⁻¹
293	-185.63
313	-163.24
333	-144.69
353	-129.10
373	-115.81
393	-104.35

procedures will be extended to the solubility of carbon dioxide in solvent mixtures of methanol and the hydrophobic ionic liquid [bmim][PF₆].

APPENDIX

Second Virial Coefficients. The influence of temperature on the second virial coefficient of pure water, $B_{11}(T)$, and pure carbon dioxide, $B_{33}(T)$, is calculated from correlation equations reported previously (Table A1; see, e.g., ref 3). These equations are based on experimental data compiled by Dymond and Smith,²¹ as recommended by Hayden and O'Connell.²²

$$\frac{B_{ii}(T)}{(\text{cm}^3 \cdot \text{mol}^{-1})} = a_i + b_i \left[\frac{c_i}{T/K} \right]^{d_i}$$

The mixed second virial coefficient $B_{13}(T)$ is calculated as proposed by Hayden and O'Connell.²² The following characteristic temperatures and pressures ($T_{c,i}$, $p_{c,i}$), molecular dipole moments (μ_i), and mean radii of gyration ($R_{D,i}$) of the pure components, as well as association parameters (η_{ij}) were used (Table A2).

Some numerical values for $B_{13}(T)$ resulting from that method at the given temperatures are given in Table A3.

Partial Molar Volume of Carbon Dioxide in Water. The partial molar volume of CO₂ (3) infinitely diluted in water (1), $v_{3,s}^\infty(T, x'_2 = 0)$, was calculated using the method of Brelvi and

Table A4

T	$v_{3,s}^{\infty}(T, x'_2 = 0)$
K	$\text{cm}^3 \cdot \text{mol}^{-1}$
293	32.66
313	33.41
333	34.65
353	36.28
373	38.30
393	40.77

O'Connell¹⁸ with the two characteristic volumes $v_3^+ = 80 \text{ cm}^3 \cdot \text{mol}^{-1}$ and $v_1^+ = 46.4 \text{ cm}^3 \cdot \text{mol}^{-1}$. For a listing of all required equations, the reader should consult ref 3. The numerical values in Table A4 result at the given temperatures.

AUTHOR INFORMATION

Corresponding Author

*Tel.: +49 631 205 2410. Fax: +49 631 205 3835. E-mail: gerd.maurer@mv.uni-kl.de.

Present Addresses

[†]BAM Federal Institute for Materials Research and Testing, D-12200 Berlin, Germany

Funding Sources

J.K. and G.M. gratefully acknowledge financial support of this investigation by Deutsche Forschungsgemeinschaft (DFG), Bonn-Bad Godesberg, Germany.

REFERENCES

- (1) Maurer, G.; Tuma, D. Gas solubility (and related high-pressure phenomena) in systems with ionic liquids. In *Ionic Liquids: From Knowledge to Application*; Plechkova, N. V., Rogers, R. D., Seddon, K. R., Eds.; ACS Symposium Series Vol. 1030; American Chemical Society: Washington, DC, 2009; pp 1–20.
- (2) Maurer, G.; Pérez-Salado Kamps, Á. Solubility of gases in ionic liquids, aqueous solutions, and mixed solvents. In *Developments and Applications in Solubility*; Letcher, T. M., Ed.; RSC Publishing: Cambridge, U.K., 2007; pp 41–58.
- (3) Pérez-Salado Kamps, Á. Model for the Gibbs excess energy of mixed-solvent (chemical-reacting and gas-containing) electrolyte systems. *Ind. Eng. Chem. Res.* **2005**, *44*, 201–225.
- (4) Pitzer, K. S. Thermodynamics of electrolytes. I. Theoretical basis and general equations. *J. Phys. Chem.* **1973**, *77*, 268–277.
- (5) Pitzer, K. S. Ion interaction approach: Theory and data correlation. In *Activity Coefficients in Electrolyte Solutions*; Pitzer, K. S., Ed.; CRC Press: Boca Raton, FL, 1991; pp 75–155.
- (6) Kumelán, J.; Pérez-Salado Kamps, Á.; Tuma, D.; Maurer, G. Solubility of the single gases carbon monoxide and oxygen in the ionic liquid [hmim][Tf₂N]. *J. Chem. Eng. Data* **2009**, *54*, 966–971.
- (7) Kumelán, J.; Tuma, D.; Pérez-Salado Kamps, Á.; Maurer, G. Solubility of the single gases carbon dioxide and hydrogen in the ionic liquid [bmpy][Tf₂N]. *J. Chem. Eng. Data* **2010**, *55*, 165–172.
- (8) Kumelán, J. Experimentelle Untersuchungen zur Löslichkeit von Gasen in ionischen Flüssigkeiten. Doctoral thesis (Doctor of Engineering), University of Kaiserslautern, Germany, 2009.
- (9) Span, R.; Wagner, W. A new equation of state for carbon dioxide covering the fluid region from the triple-point temperature to 1100 K at pressures up to 800 MPa. *J. Phys. Chem. Ref. Data* **1996**, *25*, 1509–1596.

(10) Wagner, W.; Overhoff, U. *ThermoFluids*, Version 1.0 (Build 1.0.0); Springer Verlag: Berlin, 2006.

(11) Rumpf, B.; Maurer, G. An experimental and theoretical investigation on the solubility of carbon dioxide in aqueous electrolyte solutions. *Ber. Bunsen-Ges. Phys. Chem.* **1993**, *97*, 85–97.

(12) Kumelán, J.; Pérez-Salado Kamps, Á.; Tuma, D.; Maurer, G. Solubility of CO₂ in the ionic liquids [bmim][CH₃SO₄] and [bmim][PF₆]. *J. Chem. Eng. Data* **2006**, *51*, 1802–1807.

(13) Urukova, I.; Pérez-Salado Kamps, Á.; Maurer, G. Solubility of CO₂ in (water + acetone): Correlation of experimental data and predictions from molecular simulation. *Ind. Eng. Chem. Res.* **2009**, *48*, 4553–4564.

(14) Saul, A.; Wagner, W. International equations for the saturation properties of ordinary water substance. *J. Phys. Chem. Ref. Data* **1987**, *16*, 893–901.

(15) Santiago, R. S.; Santos, G. R.; Aznar, M. UNIQUAC correlation of liquid-liquid equilibrium in systems involving ionic liquids: The DFT-PCM approach. Part II. *Fluid Phase Equilib.* **2010**, *293*, 66–72.

(16) Calvar, N.; González, B.; Gómez, E.; Domínguez, Á. Vapor-liquid equilibria for the ternary system ethanol + water + 1-butyl-3-methylimidazolium methylsulfate and the corresponding binary systems at 101.3 kPa. *J. Chem. Eng. Data* **2009**, *54*, 1004–1008.

(17) Kumelán, J.; Tuma, D.; Maurer, G. Partial molar volumes of selected gases in some ionic liquids. *Fluid Phase Equilib.* **2009**, *275*, 132–144.

(18) Brelvi, S. W.; O'Connell, J. P. Corresponding states correlations for liquid compressibility and partial molar volumes of gases at infinite dilution in liquids. *AIChE J.* **1972**, *18*, 1239–1243.

(19) Redlich, O.; Kister, A. T. Algebraic representation of thermodynamic properties and the classification of solutions. *Ind. Eng. Chem.* **1948**, *40*, 345–348.

(20) Janiczek, P.; Kalb, R.; Thonhauser, G.; Gamse, T.; Bräuer, L. Gleichgewichtskurven für Methan, Kohlendioxid und Schwefelwasserstoff in einem imidazoliumbasierten IL-Blend. Unpublished results presented at the "Jahrestreffen des Fachausschusses Hochdruckverfahrenstechnik", Maribor, Slovenia, 2011.

(21) Dymond, J. H.; Smith, E. B. *The virial coefficients of pure gases and mixtures*; Oxford University Press: Oxford, U.K., 1980.

(22) Hayden, J. G.; O'Connell, J. P. A generalized method for predicting second virial coefficients. *Ind. Eng. Chem. Process Des. Dev.* **1975**, *14*, 209–216.